Determination of the depletion layer width and effects on the formation of double-2DEG in AlGaAs/GaAs heterostructures

Irving Eduardo Cortes-Mestizo,[a] Leticia Ithsmel Espinosa-Vega, Jose Angel Espinoza-Figueroa, Alejandro Cisneros-de-la-Rosa, Eric Eugenio-Lopez, and Victor Hugo Mendez-Garcia
Center for the Innovation and Application of Science and Technology, Universidad Autonoma de San Luis Potosi, Sierra Leona 550, Lomas 4a Secc., San Luis Potosi, San Luis Potosi 78210, Mexico

Edgar Briones and Joel Briones
Departamento de Física y Matemáticas, Instituto Tecnológico y de Estudios Superiores de Occidente, Periférico Sur Manuel Gómez Morín 8585, Tlaquepaque, Jalisco 45604, Mexico

Luis Zamora-Peredo
Centro de Investigación en Micro y Nanotecnología, Universidad Veracruzana, Calzada Ruiz Cortínes 455, Boca del Río, Veracruz 94294, Mexico

Ravindranath Droopad
Ingram School of Engineering, Texas State University, San Marcos, Texas 78666

Cristo Yee-Rendon
Facultad de ciencias fisico-matematicas, Universidad Autonoma de Sinaloa, Av. de las Americas y Blvd. Universitarios, Culiacan, Sinaloa 80000, Mexico

(Received 17 November 2015; accepted 16 February 2016; published 1 March 2016)

In this work, the influence of the surface depletion layer on the formation of a two-dimensional electron gas in AlGaAs/GaAs modulated doped heterostructures is studied. The authors explore a method for estimating the depletion region inside of the GaAs-based heterostructures by using the longitudinal optical and *L*- amplitude modes observed in Raman spectra, which are supported by the modeling results. The authors found that the position of the topmost doping layer changes the electron distribution in the heterostructure and decreases the influence of the depletion layer. Similar effects are perceived when an optimized solution of $(NH_4)_2S_X$ and isopropanol is employed. The authors present a method to evaluate the formation of a double two-dimensional electron gas in a heterostructure by the adequate use of modulation line in the photoreflectance spectroscopy. © *2016 American Vacuum Society*. [http://dx.doi.org/10.1116/1.4942898]

I. INTRODUCTION

Molecular beam epitaxy (MBE), in conjunction with band gap engineering, brought to the world the high electron mobility transistor (HEMT), which was first demonstrated in 1980 at Fujitsu Labs by Mimura.[1] The first demonstration of the modulation doped and HEMT took place in AlGaAs/GaAs heterostructures where the high mobility and highly confined nature of the two-dimensional electron gas (2DEG) allowed the development of semiconductor devices that revolutionize the electronic systems.

The low temperature mobility was dramatically improved over time, leading to innovations in solid-state physics, high-frequency, and low noise electronics. Since market estimations for heterostructures show an expected increase in application and sales,[2] it is necessary to increase the mobility at room temperature by the appropriate design of the layer sequence of AlGaAs/GaAs heterostructures in order to increase the number of commercial applications. One alternative that may improve the performance of such devices is to design double-2DEG containing heterostructures (D-2DEG). These types of heterostructures are useful in the area of metrology, where it is necessary to have available a set of resistance arrays with values besides the von Klitzing constant,[3] $R_K = h/e^2$. The D-2DEG system has the advantage that the proximity position of each 2DEG allows for the controlled introduction of additional degrees of freedom associated with the third dimension.[4] The use of D-2DEG in HEMTs reduces the access resistance, increases the speed of operation of the device,[5] and exhibits lower leakage current and higher breakdown voltage as compared with the single 2DEG heterostructures.[6] Nevertheless, the formation of the D-2DEG system is still a problem in conjunction with the realization of a good matching between mobility and carriers density within each 2DEG.

Thus, the optimization of the topmost layers in heterostructures plays an important role in the examination of physics related to the interruption of the translational symmetry and the further effects on the formation of the D-2DEG.[7] For example, it has been demonstrated that the topmost atoms influence the carrier distribution and mobility of the 2DEG channels.[8] The surface and interface physics, consequently, are of considerable importance for the science and technology of the 2DEG-based devices. In this work, in order to study and decrease the surface effects on the D-2DEG containing-heterostructures, we propose the implementation of nondestructive optical spectroscopies.

[a]Electronic mail: irving.cortes@uaslp.mx

II. EXPERIMENT

The structures were grown on semi-insulating GaAs (100) substrates by MBE. Elemental sources were used in the growth chamber having a base pressure of $<5 \times 10^{-11}$ mbar using a combination of ion and cryopumping. The growth rate composition was determined using the reflection high energy electron diffraction intensity oscillation technique. For the growth of the structures used in this study, a GaAs growth rate of 0.8 monolayer/s was used. Si was used as an n-type dopant. Epiready semi-insulating GaAs substrates were used with the oxide desorption, and annealing was carried out at approximately 600 °C. Growth was initiated at 580 °C using As_4 from a valved cracker and a flux ratio of approximately 20. After the oxide-desorption process, a 100 nm thick GaAs buffer layer was grown followed by a ten periods AlGaAs/GaAs (5.6/5.6 Å) superlattice. The next layers were grown in the sequence depicted in Fig. 1. A- and B-samples were designed as single- and double-2DEG containing-heterostructures, respectively. With the intention of controlling the depletion layer width, D_L, 4.5×10^{12} cm^{-2} silicon δ-doping layers were grown at 35 and 100 nm below the surface for samples A1 and A2, respectively. Sample B1 is a symmetric double triangular quantum well with a GaAs capping layer of 25 nm. Two additional samples with a capping layer thickness of 60 ($B1_{CT=60\,nm}$) and 80 nm ($B1_{CT=80\,nm}$) were grown. Sample B2 consists of an asymmetric D-2DEG sample.[9]

Additionally, in order to modify the surface states density, sulfur treatments at room temperature were performed on samples A2 and B1. First, the samples were etched in $HCl:H_2O_2:H_2O$ (1/10/5000) for 18 s followed by a bath in $HCl:H_2O$ (1/1) for 10 s. This process cleans the surface while removing 3 nm of the capping layer.[10] The passivation process was carried out by using ammonium sulfide $(NH_4)_2S_X$ [20%] and $(NH_4)_2S_X$ [10%] diluted in deionized water, ethanol, and isopropanol.[11]

For the characterization, room temperature photoreflectance spectroscopy (PR) was carried out by employing an experimental setup similar to that described elsewhere.[12] The probe beam comes from a tungsten–halogen lamp. The laser wavelengths of 532, 405, and 325 nm with the power densities of 30, 1.6, and 15 mW/cm^2, respectively, and chopped at a frequency of 200 Hz were used as modulation sources. The Raman spectroscopy (RS) was measured in air using a Horiba Xplora plus Raman spectrometer. The excitation was supplied by the 532 nm line in a backscattering geometry in order to measure both, the longitudinal optical (LO) phonon and coupled plasmon LO phonon (L-) modes scattering in (100) orientation.[13]

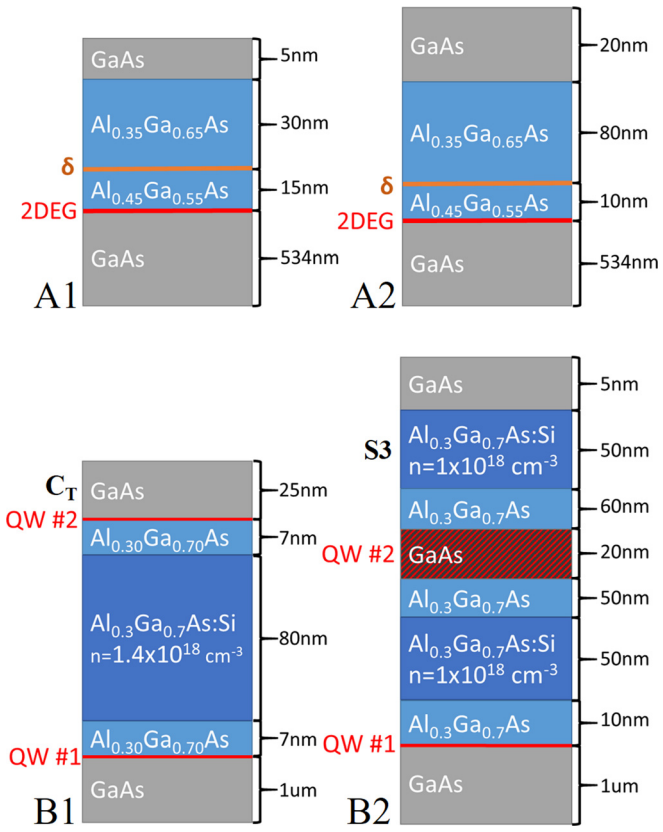

FIG. 1. (Color online) Layer sequence of heterostructures used in this work. The position of the δ-doping layer and the two-dimensional electron gas are indicated with δ and 2DEG, respectively. The B1-type samples were grown with $C_T = 25$, 60, and 80 nm. The QWs in the heterostructures are labeled as QW#1 and QW#2.

III. THEORY AND MODELING

The MBE growth process is usually realized under the As-rich conditions. Under these growth conditions, the sample surface exhibits the (2×4) and $C(4 \times 4)$ surface reconstructions, depending on the substrate temperature.[14] Prior to the removal of the samples from the high vacuum chamber, the samples are exposed at room temperature to the As molecular beam flux for several minutes, leading to a thin arsenic layer. Once the samples are taken out of the MBE system, the oxygen atoms interact with the GaAs (100) surface and a 25 Å thick outer amorphous layer, which mainly consists of Ga_2O_3 and As_2O_3 oxides, is formed.[15] Consequently, the air exposed MBE grown samples leaves an oxidized surface producing energy states at midgap.[16] When electrons migrate from their hypothetical bulk positions toward the acceptor-like low-energy surface states, the ionized host atoms lead to the formation of a D_L and the charge agglomeration in thin region of the surface, n_{SS}, which is compensated by an opposite charge inside the semiconductor, the space charge layer N_{SC}. This redistribution of charge is governed by the Poisson's equation.[17] The built in electric field close to the surface is

$$E_S = -\frac{N_{SC}\, D_L}{2\varepsilon}, \tag{1}$$

where $\varepsilon = \varepsilon_r\, \varepsilon_0$, and consequently, the voltage in that region can be described by

$$V_S = E_S \frac{D_L}{2}. \tag{2}$$

The surface barrier height, $\Phi = qV_S$, and D_L affect the formation of the D-2DEG, as will be shown later.

PR is a powerful tool to determinate E_S through the following procedure. In the PR spectra of samples usually appears damping oscillations slightly above the semiconductor band-gap energy, E_g, termed as Franz-Keldysh oscillations (FKO).[7,12,17,18] In the high electric field limit, it is demonstrated that the n-extrema of the FKO occurs when

$$n\pi = \frac{4}{3}\left[\frac{E_n - E_g}{\hbar\Omega}\right]^{3/2} + \frac{\pi}{2}, \tag{3}$$

where $\hbar\Omega$ is the characteristic electro-optic energy given by

$$\hbar\Omega = \left(\frac{q^2 E_{\text{int}}{}^2 \hbar^2}{2\mu}\right)^{1/3}, \tag{4}$$

where q is the electron charge, E_{int} is the electric field strength that produce the FKO, and μ the interband reduced mass involved in the transition. Equation (4) can be reordered as

$$E_n = \hbar\Omega\left[\frac{3\pi}{4}\left(n - \frac{1}{2}\right)\right]^{2/3} + E_g. \tag{5}$$

Thus, by plotting E_n as a function of $F_n = [(3\pi/4)(n - (1/2))]^{2/3}$, from linear fitting, we can determine $\hbar\Omega$ and E_g from the slope and the intersection with the ordinate at the origin, respectively. Recalling Eq. (4), E_{int} can be calculated by

$$E_{\text{int}} = \sqrt{\frac{2\mu(\hbar\Omega)^3}{q^2\hbar^2}}. \tag{6}$$

When the FKO associated with surface have been identified, it is possible to establish the relation $E_S = E_{\text{int}}$ and from Gauss's law $n_{SS} = \varepsilon E_S$.

The D_L can be estimated by RS using the amplitude of the peaks in the spectra.[11,13,19] In the AlGaAs/GaAs heterostructures, the laser modulation depth, d, depends on the absorption coefficient for a determined wavelength. When the condition $D_L < d$ is satisfied, two contributions of GaAs alloy to Raman scattering appear:[13,20] the LO phonon originated from D_L and the L- mode associated with scattering inside the heterostructure. D_L can be estimated by taking the RS intensities ratio $R = I(\text{LO})/I(L\text{-})$ and the relation[13]

$$R = R_0[e^{2D_L/d} - 1], \tag{7}$$

where R_0 is 1.44.[19] This estimation has a relative error of 5%–10% due to the measurement process,[13] the transition region between the D_L and the bulk,[20] the presence of the D_L inside the AlGaAs layer, and by the slight increase of d in the ternary in contrast with GaAs.

In order to compare the experimental results with the theoretical values, we employed a commercial available technology computer aided design (TCAD) software. In the model, the equation of Schrödinger–Poisson is solved by taking into account two energy levels of surface states, which consist of a deep donor and one deep acceptor levels, as in Ref. 16. The layer sequence of the heterostructures in Fig. 1 was modeled in one-dimension in order to get the band profile and in the two-dimensional mode with the aim to calculate the electron distribution in the samples.

IV. RESULTS AND DISCUSSION

A. Control of the D_L by a doping layer

In a typical PR spectra of AlGaAs/GaAs heterostructures, three regions of oscillations at 300 K can be identified. Region I, between 1.3 and 1.45 eV, is associated with the AlGaAs/GaAs interface where the 2DEG is formed.[21] Region II, from 1.45 to 1.8, presents FKO produced by E_S as described previously.[22] Above 1.8 eV, oscillations or transitions related to AlGaAs might occur,[12] depending on the aluminum fraction in the ternary. Figure 2(a) shows the PR spectra of the A-samples. FKO in region II are missing for A1 but appear for sample A2, and for which $E_S = 2.9 \times 10^7$ V/m.

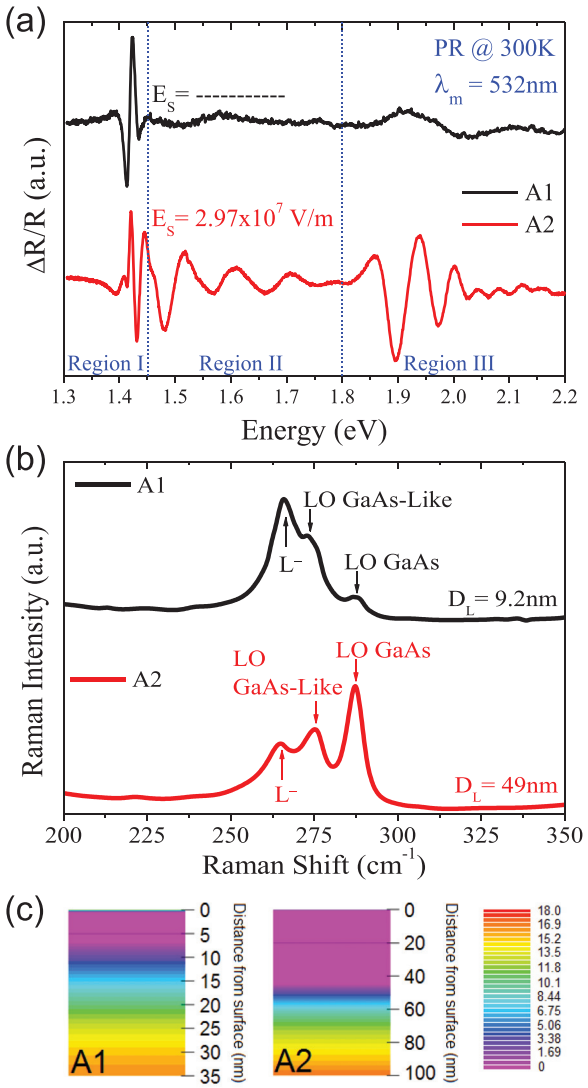

FIG. 2. (Color) (a) PR of A-samples, where the presence/absence of oscillations in region II is illustrated. (b) RS of A1 and A2. The intensity ratio of LO and L- mode is modified by the width of the depletion layer. (c) Electron concentration (cm^{-3}, in logarithmic scale) in the two topmost layers for the A-samples.

The presence of FKO in A2 are due to photogenerated minority carriers that recombine with the charge trapped in surface states reducing E_S and changing the reflection coefficient. The proximity of the δ-doping layer to the surface contributes to short D_L for A1. Therefore, the high field region is so thin that the incident light barely sees the depletion region not allowing for the modulation with the laser.[23] Similar behavior was reported by Hsu *et al.*[23] They placed a δ-doping layer at different depths from surface ranging from 250 to 25 nm and found FKO for all samples except for the 25 nm sample, due to the short value of D_L.

In order to determine D_L in the A-samples, we analyzed the RS of A1 and A2 shown in Fig. 2(b). Three peaks are present: LO, LO GaAs-like, and *L*- located at 287.26, 275.14, and 265.94 cm^{-1}, respectively. By using the formalism depicted in Sec. III, through the ratio R, the D_L was calculate to be 9.25 and 49 nm for A1 and A2, respectively. The small D_L for A1 is due to the position of the δ-doping near to the surface that contributes to filling the surface states producing a short depletion layer; this result confirms the PR observations that in a short D_L, the modulation process is not carried out. In Fig. 2(c), the calculated spatial distribution of electrons by the TCAD model in the capping and barrier layer of A-samples is presented. The D_L goes from $\sim$0 e/cm^3 in the GaAs capping layer (purple color) to 10^3 e/cm^3 into the AlGaAs barrier layer (dark purple color). This lack of electrons was found at the depth of 10 nm for A1 and 50 nm for A2, which agrees and validates the values determined by Raman spectroscopy.

In Fig. 3, the PR spectra of samples B1 for which the capping layer thickness was increased from 25 to 80 nm are presented. It is observed that as the thickness of the capping layer, C_T, is increased, the period of the FKO decreases. As C_T gets thicker, it increases the distance of the doped AlGaAs barrier layer to surface, producing a similar effect on the A-samples studied. The n-extreme of the FKO in the samples (labeled with letters) shifts toward low energies by the reduction of the electric field at the surface from 3.0×10^7 to 1.4×10^7 V/m as the capping layer changes from 25 to 80 nm. This behavior indicates that the reduction in the FKO period is not produced by the δ-doping, as in the case of the A-samples and Ref. 23, but it is related to the reduction in the migration of electrons from the highly doped barrier layer toward the low energy states at the surface. Accordingly, n_{SS} decreases from 2.18 to 1.06×10^{12} e/cm^2 when the C_T changes from 25 to 80 nm. Nevertheless, even when n_{SS} diminishes with the thickness of the capping, we found that D_L increases from 47 to 90 nm for the same range of C_T.

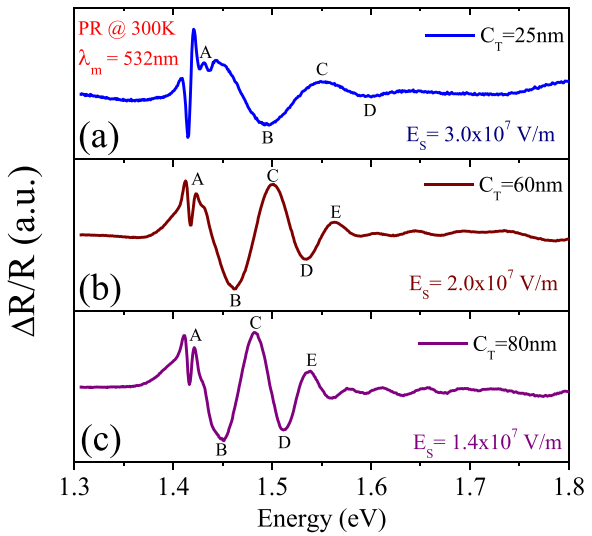

FIG. 3. (Color online) PR spectra of B1 with capping layers of (a) 25 nm, (b) 60 nm and (c) 80 nm. The n-extrema of the FKO associated with surface is labeled with capital letters. A mixing between the region I and II oscillations is observed.

B. Control of the D_L by passivation process

Sulfur treatment of the GaAs surface has been one of the most explored techniques to passivate the GaAs.[11,13,19] This process produces a surface that is free of dangling bonds prohibiting the chemical absorption[24] and reducing the surface state density.[11] Poor acceptor-like surface with small n_{SS} sustains the small intensity of E_S and short D_L. The effect of the passivation on the AlGaAs/GaAs heterostructures is shown in Fig. 4(a) for sample A2. In this figure, the RS is presented prior to and after the passivation treatment, employing a solution of $(NH_4)_2S_X$ with isopropanol as solvent. The intensity of the LO mode in RS after the passivation process decreases and is an indication that the depletion layer has been reduced by the modification of the surface states. This demonstrates that even for heterostructures, the LO photon is sensitive to the modification of the surface depletion layer as it is in bulk materials. As a result of the passivation for A2, D_L changes from 49 to 33 nm.

The passivation method is enhanced when the $(NH_4)_2S_X$ is diluted in low dielectric constant solvents as is summarized in Fig. 4(b) for sample A2. The D_L changes from 49 nm in the as-grown sample to a 33 nm after the surface passivation with intermediate values when the dielectric constant of the solvent was varied in the passivation solution. The dependence of D_L with the dielectric constant of the passivation solution was studied by Bessolov *et al.* for bulk GaAs surface.[11] They explain the phenomena to be a result of an exponential increase in the rate constant of the reaction of the sulfur coat formation. The passivation method for heterostructures exposed in this work conduces to similar results reported in Ref. 11 for bulk GaAs. Therefore, these surface treatments could be very useful for those cases where the surface states strongly affect the 2DEG.

C. Effect of D_L on the 2DEG formation

By the variation of the modulation source wavelength, λ_m, in PR, it is possible to evaluate the origin of the spectra signatures from the different interfaces in the heterostructures.[12] For example, the UV laser $\lambda_m = 325$ nm is able to explore the topmost layers of the heterostructure, due to its low d in GaAs.[7,25] Therefore, the UV line is especially useful to study the B-samples designed as D-2DEG since it is necessary to discriminate the information coming from

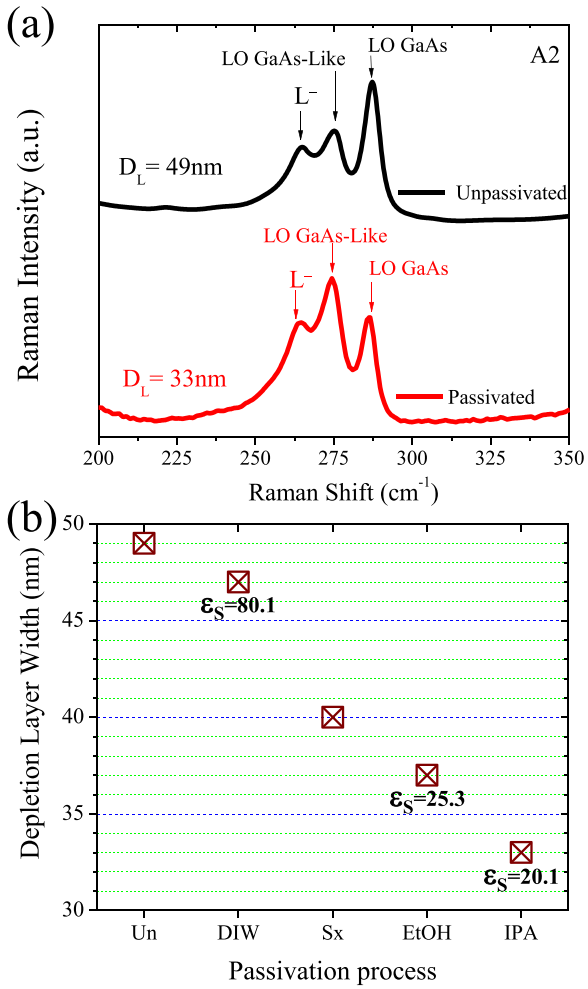

FIG. 4. (Color online) (a) RS of A2 before and after the passivation treatment. The reduction of the LO mode indicates that the passivation procedure has been successfully applied. (b) D_L as a function of the passivation procedure: unpassivated (*Un*), passivated in pure $(NH_4)_2S_X$ (*Sx*), and passivated in $(NH_4)_2S_X$ diluted with deionized water (DIW), ethanol (EtOH), and isopropanol (IPA). The dielectric constant of the solvent, ε_s, is indicated (Ref. 11).

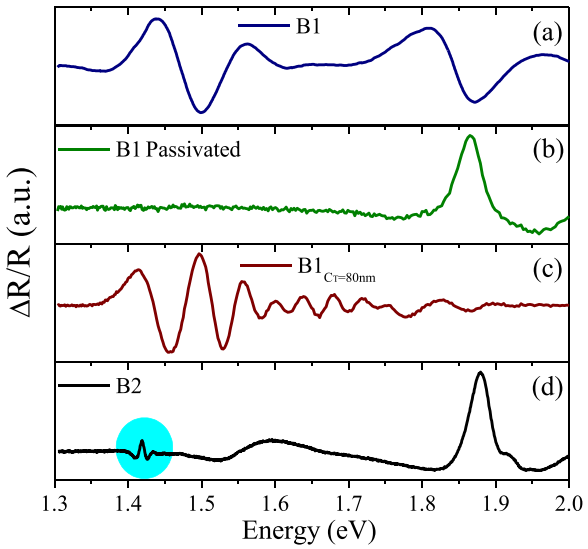

FIG. 5. (Color online) PR measurements taken with a short laser modulation line from samples (a) B1, (b) B1 after the passivation method, (c) $B_{CT=80\,nm}$, and (d) B2-sample. The oscillations associated with the formation of the 2DEG in QW#2 are highlighted in the shadow area.

topmost- and deeper-layers. In Fig. 5(a), the PR of B1 is shown with a $\lambda_m = 325$ nm, and the total d is $\sim$100 nm for this laser.[26] We notice that the FKO associated with the surface electric fields dominate the spectra and the E_S was calculated to be 3.5×10^7 V/m. This value is slightly higher than the intensity determined by measuring with $\lambda_m = 532$ nm laser. The variation is caused by the differences in the power of the laser beams.[23] Even when the FKO in region II of the Fig. 3(a) dominate the spectra, the oscillations in region I appear because of the larger d of the $\lambda_m = 532$ nm laser. Thus, by employing $\lambda_m = 532$ nm, it was possible to modulate the electric fields located deeper in the structure, as those lying in the 2DEG interface of quantum well (QW)#1. Therefore, the absence of oscillations in Fig. 5 from region I when employing the line $\lambda_m = 325$ nm indicates that the topmost 2DEG is not formed for the B1 sample. As shown in Fig. 5(b), after sample B1 passivation process, the PR neither exhibits oscillations in region I nor in region II. Then, despite that E_S has been decreased, the surface states still hinder or forbid the formation of the 2DEG in QW#2. An additional evidence of the successful implementation of passivation procedures is demonstrated in the spectra of Fig. 5(b), since it is worth to note that there is no FKO oscillations in region II, attributed to the surface electric field strength reduction. In other words, E_S was reduced below 1.7×10^7 V/m, strength less than the intermediate field intensity where the FKO may be present.[12]

As in the case of the sample B1 before the passivation process, the PR spectra of $B1_{CT=80}$ with $\lambda_m = 325$ nm shows FKO in region II, even though the oscillations originated at the 2DEG are not exhibited. This is induced by the larger D_L (of 90 nm) in the heterostructure, superior value than the distance from surface to QW#2. The same behavior in the PR is shown by the $B1_{CT=60}$ sample. Even when the distance from the surface has been increased, D_L still affects the formation of a 2DEG in the QW#2 in this set of samples, as will be shown.

As presented in the layered structure of Fig. 1, QW#2 in sample B2 is located at a larger distance from the surface as compared with B1. Then, we used an additional modulation line of 405 nm to explore B2, which is shown in Fig. 5(d). The PR spectra of sample B2 exhibit small amplitude oscillations in region I, indicating the formation of a 2DEG in QW#2. It is also observed that FKO are absent in region II, which is attributed to the reduction in D_L by the presence of the AlGaAs n-type layer, labeled as S3 in Fig. 1.

Numerical analyses of the conduction band profile, C_B, of the B-samples were performed in order to get comprehensive understanding of the effects of D_L on the formation of the topmost 2DEG and corroborate that with the presence of the oscillation in region I as an indication of the formation of the 2DEG. Figure 6 shows TCAD simulations of C_B of samples B. The red line corresponds ideal conduction band profile for sample B1, i.e., without any disturbance of the surface states. In this case, the surface states density does not affect the carrier distribution in the device, and the band bending close to

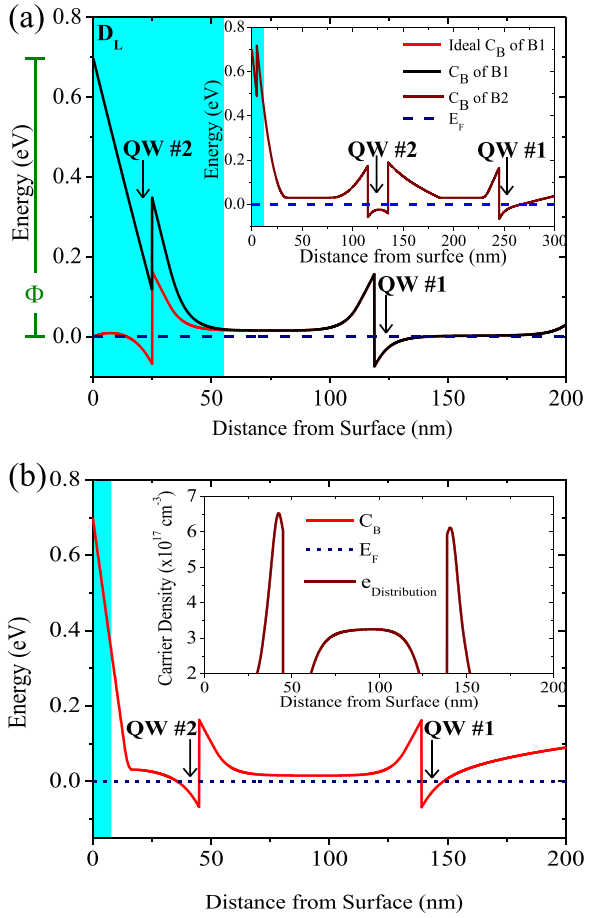

FIG. 6. (Color online) (a) Simulation of the conduction band profile, C_B, for the ideal case of sample B1 (red line) and considering the population of surface states (black line). In the inset, the C_B profile of sample B2 is plotted. (b) C_B bending for B1 considering a δ-doping in the cap layer. The carrier distribution is shown in the inset. D_L is indicated in the shadow area.

the surface is barely perceived. As a consequence, QW#2 lies under the Fermi level (dotted line), and the formation of the 2DEG is possible. In the case where the filling of the surface states is considered, $n_{SS} = 2.1 \times 10^{12}\,\mathrm{cm}^{-2}$, a $\Phi = 0.7\,\mathrm{eV}$ is formed at the surface, and a significant band bending occurs, pulling the QW#2 out of the Fermi level, avoiding the formation of the 2DEG. After the passivation process, the RS analysis indicates that D_L in B1 is 30 nm, so the position of QW#2 is still inside D_L, not allowing for the formation of a 2DEG. On the other hand, the C_B for B2 is shown in the inset of Fig. 6(a). According to RS for B2, the doping layer S3 reduces the influence of the surface on the topmost layers contributing to a D_L as thin as 11 nm. As observed in the inset of Fig. 6(a), the near surface band bending now occurs in a narrow region, allowing the formation of a D-2DEG system, since both of the QWs are below the Fermi level. The concept of isolating the effect of the surface and reducing D_L by a doping profile is explored by numerical simulation of B1 layer sequence on Fig. 1 with $C_T = 45$ nm and a δ-doping profile of $4.5 \times 10^{12}\,\mathrm{cm}^{-2}$ collocated at 15 nm from surface, the result of which is illustrated in Fig. 6(b). The simulation indicates that D_L is $\sim$13 nm and, as in the case of B2, this short value does not disturb the formation of a 2DEG in QW#2. In this case, the layer of a δ-doping profile presents a lower mobility in comparison with the linear profile in the S3 layer of sample B2 at room temperature, making this concept useful to reduce the parasitic current in heterostructures. In the inset of Fig. 6(b), the carrier concentration in the quantum wells is analyzed. The electron concentration is 6.1 and $6.5 \times 10^{17}\,\mathrm{cm}^{-3}$ for the 2DEG in QW#1 and QW#2, respectively. Thus, there is a $\sim$7% of mismatch of carrier concentrations of the 2DEG between one QW and the other. This value can be tailored by varying the position and density of the δ-doping. The numerical analysis in Fig. 6 confirms that only the B2 sample can be considered as a D-2DEG system since only in this heterostructure the QW#2 lies under the Fermi level. This analysis agrees with the fact that only the B2 sample shows oscillations in region I. Thus, when the first layer of the B-samples are explored by PR with a short modulation line, oscillations in region I appear only when the formation of the topmost 2DEG occurs, as in the case of the single 2DEG samples.[22,26]

V. SUMMARY AND CONCLUSIONS

In this work, the electric field and depletion region of AlGaAs/GaAs heterostructures were measured by optical spectroscopies and compared with theoretical modeling. The photoreflectance spectroscopy is a powerful tool to determine the electric field intensity. However, when the depletion region close to the surface is small or the intensity of E_S lies in the low field limit, it is not possible to evaluate their intensity. The relationship between the LO and L- mode in the RS of GaAs-based heterostructures allows for the determination of D_L. The D_L depends on the position where the doping layer in the heterostructures is located and passivation procedures used with $(NH_4)_2S_X$ based solutions. The sulfur treatment is more efficient when a low dielectric constant solvent is used. If a quantum well lies inside the depletion region, the formation of a 2DEG is not possible. Henceforth, with the formation of the topmost 2DEG, oscillations in region I of the PR spectra occurred even for short laser penetration lengths. Therefore, a PR analysis allows us to evaluate the formation of a D-2DEG system, without the use of more expensive and complexes characterization techniques such as the quantum Hall effect.

ACKNOWLEDGMENTS

The authors acknowledge the financial support from CONACYT-Mexico through Grant No. CEMIESOL-22, Fondo de Infraestructura 2015-255489, PNCPN2014-01: 248071, Inmersion a la Ciencia-UASLP, and FAI-UASLP.

[1]T. Mimura, IEEE Trans. Microwave Theory Tech. **50**, 780 (2002).
[2]G. Fiori, F. Bonaccorso, G. Iannaccone, T. Palacios, D. Neumaier, A. Seabaugh, S. K. Banerjee, and L. Colombo, Nat. Nanotechnol. **9**, 768 (2014).
[3]A. Bounouh, W. Poirier, F. Piquemal, G. Genevès, and J. P. André, IEEE Trans. Instrum. Meas. **55**, 555 (2003).
[4]G. S. Boebinger, H. W. Jiang, L. N. Pfeiffer, and K. W. West, Phys. Rev. Lett. **64**, 1793 (1990).
[5]T. Palacios, A. Chini, D. Buttari, S. Heikman, A. Chakraborty, S. Keller, S. P. DenBaars, and U. K. Mishra, IEEE Trans. Electron Devices **53**, 562 (2006).
[6]A. Zanandra *et al.*, Microelectron. Reliab. **52**, 2426 (2012).

[7]L. Zamora-Peredo, I. E. Cortes-Mestizo, L. García-González, J. Hernández-Torres, D. Vázquez-Cortes, S. Shimomura, A. Cisneros-delaRosa, and V. H. Méndez-García, J. Cryst. Growth. **378**, 100 (2013).
[8]X. Z. Dang, E. T. Yu, E. J. Piner, and B. T. McDermott, J. Appl. Phys. **90**, 1357 (2001).
[9]K. Pierz, G. Hein, B. Schumacher, E. Pesel, and H. W. Schumacher, Semicond. Sci. Technol. **25**, 035014 (2010).
[10]S. Sioncke, D. P. Brunco, M. Meuris, O. Uwamahoro, J. Van Steenbergen, E. Vrancken, and M. M. Heyns, ECS Trans. **16**, 451 (2008).
[11]V. N. Bessolov, M. V. Lebedev, and D. R. T. Zahn, J. Appl. Phys. **82**, 2640 (1997).
[12]J. Misiewicz, P. Sitarek, G. Sek, and R. Kudrawiec, Mater. Sci. (Poland) **21**, 263 (2003).
[13]X. Chen, X. Si, and V. Malhotra, J. Electrochem. Soc. **140**, 2085 (1993).
[14]A. Ohtake, Surf. Sci. Rep. **63**, 295 (2008).
[15]V. L. Berkovits, A. B. Gordeeva, and V. A. Kosobukin, Solid State Commun. **119**, 647 (2001).
[16]K. Horio and T. Yamada, IEEE Trans. Electron Devices **46**, 648 (1999).
[17]R. E. Wagner and A. Mandelis, Phy. Rev. B **50**, 14228 (1994).
[18]H. Shen and F. H. Pollak, Phy. Rev. B **42**, 7097 (1990).
[19]L. A. Farrow, C. J. Sandroff, and M. C. Tamargo, Appl. Phys. Lett. **51**, 1931 (1987).
[20]A. Pinczuk, A. A. Ballman, R. E. Nahory, M. A. Pollack, and J. M. Worlock, J. Vac. Sci. Technol. **16**, 1168 (1979).
[21]O. J. Glembocki, B. V. Shanabrook, N. Bottka, W. T. Beard, and J. Comas, Appl. Phys. Lett. **46**, 970 (1985).
[22]C. R. Lu, C. L. Chang, C. H. Liou, J. R. Anderson, D. R. Stone, and R. A. Wilson, Appl. Surf. Sci. **92**, 404 (1996).
[23]T. M. Hsu, Y. C. Tien, N. H. Lu, S. P. Tsai, D. G. Liu, and C. P. Lee, J. Appl. Phys. **72**, 1065 (1992).
[24]Y. Nannichi, J. Fan, H. Oigawa, and A. Koma, Jpn. J. Appl. Phys., Part 2 **27**, L2367 (1988).
[25]L. Pavesi and M. Guzzi, J. Appl. Phys. **75**, 4779 (1994).
[26]M. Sydor, N. Jahren, W. C. Mitchel, W. V. Lampert, T. W. Haas, M. Y. Yen, S. M. Mudare, and D. H. Tomich, J. Appl. Phys. **67**, 7423 (1990).

Copyright of Journal of Vacuum Science & Technology: Part B-Nanotechnology & Microelectronics is the property of AVS, The Science & Technology Society and its content may not be copied or emailed to multiple sites or posted to a listserv without the copyright holder's express written permission. However, users may print, download, or email articles for individual use.